

Identifying damage on cars through the integrated use of TLS/SfM with thermographic images

V. Barrile, G. M. Meduri, G. Bilotta

Abstract—The laser scanner is a detection technique essential for the 3D modeling of objects and it is well known its capability to acquire large amounts of data relatively in short times with a high degree of precision. In recent years also it is becoming more common some software-based algorithms "Structure from Motion" (SfM) which allow the graphic rendering of 3D models from images obtained by ordinary digital cameras.

The integration of the 3D model with images obtained with infrared cameras can provide an overview not only on the state of conservation, but also provide, in addition to the dimensional characterization, also abnormality information, dimensional and form, invisible to human eyes and to other techniques.

In particular, this application with the integrated use of terrestrial laser scanning instrumentation and advanced infrared camera can test a possible use for cars, after packaging and transport, in order to detect any damage caused by transport. We also will conduct the first tests on a possible use of the SfM to replace laser scanner

Keywords—3D modeling, Advanced Infrared camera, Laser scanner, Thermography.

I. INTRODUCTION

THE integration between a three-dimensional digital model, realized by scanning laser terrestrial systems, and the radiometric information, obtained by advanced infrared camera, allows to investigate, also to a high degree of detail, some particular characteristics of an object at very different dimensional scales, resulting in what is called in the literature *Texture mapping*. Using *target* [1]–[2], thermo-rendered recognizable, it was possible to perform the texturing of the virtual models with IR images, thus obtaining the integration between spatial and radiometric data. There are also techniques that allow the generation of 3D models from pictures taken with common digital cameras, through the use of dedicated software-based algorithms "Structure from

Motion" (SfM); It is therefore a fundamental evaluation of the results obtained compared with the use of laser scanners.

II. OPERATIONS AND TRACKING MODE

The integration between geometric and spectral data enable to extract quantitative information concerning the extension of thermal anomalies or special events that take place within a historical artefact or a modern opera [3]. To perform this procedure is generally required to manually identification of homologous points between 3D model and 2D image [4]. The method that permits using the pairs of points identified is Direct Linear Transformation defined, DLT. To allow the reconstruction of geometric model, first, and texturing, after, is necessary to know the orientation parameters inside of the tools used [5], known and physically and rigidly tying the tools it has been possible consider constant the roto-translation between them. It was therefore possible to consider a global reference system, and referring the orientation of the thermal chamber relative to the internal reference of laser scanner through a physical and rigid bond between the instruments with a steel bar. After identifying which surface of the car acquire and textured, you place the target (minimum three), which are the points of support of the georeferencing of the point clouds and images (both thermal and radiometric) on the virtual model. It is therefore necessary to study the most suitable and homogeneous distribution on the area to be investigated, in order to ensure an equally homogeneous projection of the image on model. The targets, moreover, can be preferentially arranged especially in areas with greater undulation of the surface, so as to achieve greater accuracy, reducing the errors due to the geometric distortion of the scene arising from a not good recording of 2D data (images) and 3D data – point cloud or mesh [6].

The target, in addition to allowing the roto-translation of point clouds acquired in the same reference system, allow the texturing of the images on the three-dimensional global model. The signals used in this study are highly reflective and retro-reflective signs, measuring 3" x 3" used for high-resolution scans of detail (laser scanner Leica HDS 3000). We detected and calculated the center of these signals semi-automatically with the software implemented in the instrument that associates to the center of gravity of the signal in the point cloud the respective coordinates in a reference system with

V. Barrile is with the DICEAM Department, Faculty of Engineering Mediterranean University of Reggio Calabria, Reggio Calabria 89100 IT (phone: +39-0965-169-2301; e-mail: vincenzo.barrile@unirc.it).

G. M. Meduri is with the DICEAM Department, Faculty of Engineering Mediterranean University of Reggio Calabria, Reggio Calabria 89100 IT (email: ing.giuseppemariameduri@gmail.com).

G. Bilotta was with the Department of Planning, IUAV University of Venice, Venice 30135 IT. She now collaborates with the DICEAM Department, Faculty of Engineering Mediterranean University of Reggio Calabria, Reggio Calabria 89100 IT (e-mail: giuliana.bilotta@iuav.it).

origin in the center of the instrument [7]. The surface is then scanned with a laser scanner type Leica HDS 3000: a laser time of flight (TOF Time of Flight) that allows to acquire in a few minutes the three-dimensional coordinates of large quantities of points distributed on the surface in question according to a regular grid. To get coverage of the entire surface, thus limiting the areas or items in shadow, were usually also acquired even more point clouds of the same area.

When the scan surface scans are carried out in detail, with the same Leica HDS 3000, centered on each of the target on the surface: the signals are manually identified on the point cloud and acquired by the instrument which, in the end, automatically identifies the target scanned. The uncertainty in the calculation of the coordinates of the target depends on the uncertainties and mistakes of the laser scanner. In order to be univocally recognized in the thermal image and to perform in this way a correct texturing, it is necessary that the targets are also thermally visible, and then chromatically recognizable, compared to the context of the surface in which they are located. For this reason they have been sprayed with a spray cold, or dry ice. It is a phase to be performed with a certain speed, since the effect of instantaneous cooling of the signal has a rather short duration in time (few minutes).

It is also important that the sizes of the vaporized area are as small as possible, so that the corresponding area on the relative IR image is equally limited by avoiding to affect the final result. Then an acquisition is made with thermal imaging camera (Reference image) initially with a single outlet in automatic mode to highlight the range of temperatures recognized. It is more convenient to acquire a greater number of thermal images to cover the entire surface rather than acquiring a single image, especially in the case of surfaces structurally complex, considering also the lower sensitivity of the detector with increasing distance.

III. DATA PROCESSING

The process of data processing can be summarized in the following steps:

- Alignment of point clouds
- Meshing point clouds
- Calibration procedure
- Texturing infrared

To record the clouds and generate the whole cloud, each time was used the ICP algorithm (Iterative Closest Point) implemented in the Matlab environment.

The ICP algorithm iteratively applied a rigid roto-translation in one of the two clouds, considered mobile, so that overlap in the best possible way to another cloud, considered fixed.

Given a point cloud V^j and a point cloud V^i to align with each other, for each y_i point of V^j , exists at least one x_i point on the cloud V^i , called corresponding point, which is the closest to y_i compared to all other points in X .

The algorithm is an efficient method to tackle rigid registration between two point sets. Its goal is to find a rigid transformation, with which Y is registered to be in the best

alignment with X , that is, let T of Equation:

$$\min_{T, j \in \{1, 2, \dots, N_x\}} \left\{ \sum_{i=1}^{N_y} \left\| T(y_i) - \vec{x}_j \right\|_2^2 \right\} \quad (1)$$

be rotation and translation transformations, hence the rigid registration between two point sets is

$$\min_{R, t, j \in \{1, 2, \dots, N_x\}} \left\{ \sum_{i=1}^{N_y} \left\| (R y_i + t) - \vec{x}_j \right\|_2^2 \right\} \quad (2)$$

$$\text{s.t. } R^T R = I_x; \det(R) = 1$$

In an iteration, ICP assumes that the closest points correspond, computes the absolute orientation and applies the resulting rigid transformation to V^j . In practice, at step 1 for each point of mobile cloud (V^j set), are sought, within the fixed point cloud, the points (closest points) contained in a sphere of a certain radius (multiple of a parameter introduced by user) belonging to V^i set. The closest of these will be held and considered the corresponding point.

$$C_k(i) = \arg \min_{j \in \{1, 2, \dots, N_x\}} \left\{ \left\| (R_{k-1} y_i + t_{k-1}) - \vec{x}_j \right\|_2^2 \right\} \quad (3)$$

With these matches found, in step 2, the algorithm computes the incremental transformation (rotation matrix $R_{i,j}$ and translation vector T and solving the absolute orientation) by applying it to the elements of V^j ; If the Mean Squared Error is less than a certain threshold, the iteration terminates otherwise return to step 1;

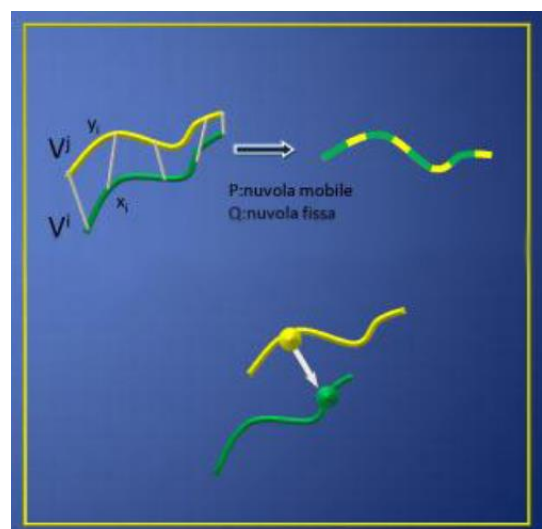


Fig. 1 Iterative closest point

$$(R_k, t_k) = \arg \min_{R^T R = I_m, \det(R)=1, t} \left\| \left(\begin{matrix} \vec{R} y_i + t \\ \vec{R} y_i + t \end{matrix} \right) - \vec{x}_{c_k(i)} \right\|_2^2 \quad (4)$$

The principle on which is based this algorithm is that the alignment between the two point clouds corresponds to the minimization of the quadratic error of the minimum distances between the two objects. In fact, Besl and McKay demonstrated that the algorithm converges to a local minimum of the error (Fig. 6).

$$e = \sum_{i=1}^N \|x_i - (R y_i - T)\|^2 = \min \quad (5)$$

$$C: V^j \rightarrow \frac{V^i}{V^j} \in V^j \exists x \text{ such that } \min \text{ distance } (y, x) < \sigma \quad (6)$$

Therefore, we transformed the point cloud into virtual surfaces of *mesh* type, in most cases forming triangles of irregular shape. For this operation, we used *software MeshLab environment*.

MeshLab is an open source software widely used in the field of 3D modeling and treatment of large amounts of data as coordinates or point clouds. Its purpose is to treat, organize and process data generated by 3D scanners, offering tools to edit, clean and simplify point clouds obtained. This software was developed in Italy in the research center ISTI - CNR for the University of Pisa in 2005.

The process of reconstruction of a surface from a point cloud generally follows some steps:

The first step is to clean up the point cloud from unnecessary data; this may take a long time since it must be done manually through the selection tool, but it is of fundamental importance because the presence of items not belonging to the object can generate unnecessary geometry that alter the shape of the model.

In some cases, in addition to the operation of removal of the undesired points it might also be necessary to carry out operations of simplifications in order to reduce the calculation time, and of smoothing in order to reduce any noise in the data.

Finally, for the reconstruction of the surface we use the command Poisson. This tool allows, starting from a point cloud, of reconstructing a digital replica of the object detected. In fact, after setting parameters, the filter will close the open parts and will generate triangles that compose the 3D model.

The accuracy of the reconstruction depends on 4 parameters: *Octree Depth*, *Solver Divide*, *Samples per Node*, *Surface Offsetting*.

- *Octree Depth* determines the precision with which we will carry out the reconstruction of the surface, the higher the value, the more the surface will be detailed. The

increase of this parameter leads to an increase in computation time.

- *Solver Divide* allows a reduction of the resources needed for the calculation of the area, but at the cost of an increase of the times. For values of *Octree Depth* greater than 8, a value of *Solver Divide* of 7 or 8 may decrease memory usage during the calculation of the surface
- *Samples per Node* is a parameter whose optimum value depends on the amount of noise present in the point cloud. A higher value of this parameter allows smoother surfaces, and thus more insensitive to noise. In the case of point cloud with little noise, a lesser value of the *Samples for Node* allows to obtain a more detailed surface.
- *Surface offsetting* is a correction index whose value can vary between 0.5 and 2. A value of 1 indicates that there is no offset.

The values to be assigned vary from case to case, and to determine those that produce the best results it is necessary to perform the tests. In general, however, a higher value of the parameter *Octree Depth* determines a more detailed surface.

After rebuilding the surface, we can simplify it. The process is called decimation and is used to reduce the number of triangles of which is formed the surface. This can be useful, for example, when the surface is used to perform a 3D printing process that requires very long times in the case of complex surfaces. For simplification, we can use the command *Quadric Edge Collapse Decimation*. We can define the number of triangles of which will be formed the surface after the decimation or the percentage reduction. A greater number of triangles determines a surface more detailed, while a smaller number of triangles determines a surface easier to analyze. The right balance obviously depends on the purpose and the computational possibilities.

Another approach to align the camera images with the scanner coordinate system is to use a calibration procedure. Each camera has unique parameters that define how a point (X,Y,Z) in world coordinates is projected onto the image plane. These parameters are calculated through a process known as geometric camera calibration. Given the focal length (f_x, f_y) of the camera and the camera center (c_x, c_y), image coordinates (x,y) are calculated as:

$$\begin{bmatrix} x \\ y \\ 1 \end{bmatrix} = \begin{bmatrix} f_x & 0 & c_x \\ 0 & f_y & c_y \\ 0 & 0 & 1 \end{bmatrix} \begin{bmatrix} X/Z \\ Y/Z \\ 1 \end{bmatrix} \quad (1)$$

Given the radial distortion coefficients k_1, k_2, k_3 and the tangential distortion coefficients p_1, p_2 and $r = \sqrt{x^2 + y^2}$ the corrected image points (x_c, y_c) are calculated as:

$$\begin{pmatrix} x_c \\ y_c \end{pmatrix} = \begin{pmatrix} x(1 + k_1 r^2 + k_2 r^4 + k_3 r^6) + 2p_1 y + p_2(r^2 + 2x^2) \\ y(1 + k_1 r^2 + k_2 r^4 + k_3 r^6) + p_1(r^2 + 2y^2) + 2p_2 x \end{pmatrix} \quad (2)$$

Once all the points are, in the camera coordinate system, the projection to the image can be defined up to a factor s using equation (3):

$$s \begin{bmatrix} x \\ y \\ 1 \end{bmatrix} = \begin{bmatrix} f_x & 0 & c_x \\ 0 & f_y & c_y \\ 0 & 0 & 1 \end{bmatrix} \begin{bmatrix} r_{11} & r_{12} & r_{13} & t_1 \\ r_{21} & r_{22} & r_{23} & t_2 \\ r_{31} & r_{32} & r_{33} & t_3 \end{bmatrix} \begin{bmatrix} X \\ Y \\ Z \\ 1 \end{bmatrix} \quad (3)$$

The maximum likelihood estimate of the transformation between the scanner and camera coordinate system is obtained by minimizing:

$$\sum_{i=1}^n \sum_{j=1}^m \|\mathbf{p}_{ij} - \hat{\mathbf{p}}(\mathbf{A}, \mathbf{D}, \mathbf{R}_i, \mathbf{t}_i, \mathbf{P}_j)\|^2 \quad (4)$$

where n is the number images of the calibration pattern, m planar points on the pattern A is the camera calibration matrix, R_i the rotation matrix, t_i the translation vector, and D the distortion parameters.

$\hat{\mathbf{p}}(\mathbf{A}, \mathbf{D}, \mathbf{R}_i, \mathbf{t}_i, \mathbf{P}_j)$ defines the projection of point P_j in image i , according to equation (3) and (2).

This approach assumes that we have a number of points identifiable in both the laser scan and the image.

Finally, in *RapidForm* environment, the infrared image is textured on the *mesh*, using as support points the *target laser scanning* on the real surface. Having made the *target* thermally recognizable, with the dry ice we made the same as a distinct color in the image, corresponding to a temperature much colder compared to the context in which they are found. Thermal infrared cameras for building, as the one used, hardly have higher resolution than 640 x 480 pixels, this justifies the uncertainty of higher values than those in the visible. Performing the texturing using multiple points of support, even if not recognizable automatically by the *laser scanner*, the result would be very good. Nevertheless, not being able to cover the surface of study with a high number of targets for practical matters-operational and in order not to generate additional shadow zones, we should always get a good compromise between target number for image and final quality of the textured model.

Because we used the laser scanner with a digital camera inside, we also wanted to explore the use of SfM, by using the images captured by the instrument during scans; SfM is in fact a recent technique that allows getting a 3D model from simple digital images produced by common cameras.

The flow chart in Fig. 2 shows the workflow, starting from the digital images, yields to the 3D structural model.

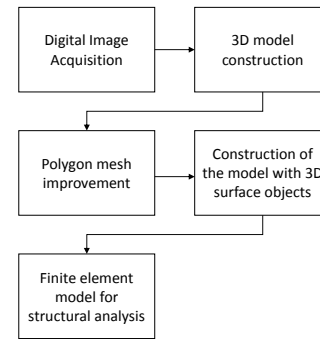


Fig. 2 Workflow for transition from photogrammetric 3D survey to a structural model

The procedure of photographs processing and 3D model construction comprises four main steps.

1. The first phase is the alignment of the camera. At this step, PhotoScan seeks common points on the photographs to merge with each other through the identification of a matching camera for every image and parameters of aging and calibration. As a result, they form a cloud of scattered points and a series of shots.

2. The next phase is the construction of dense point cloud. Based on the positions of recovery estimated and extracted from the photos, PhotoScan generates a point cloud more dense and detailed. We can modify and classify this point cloud before proceeding with the export or the generation of three-dimensional mesh model.

3. Then we proceed with the construction of the mesh. PhotoScan reconstructs the surface of a 3D polygon mesh representing the object based on the dense point cloud obtained from the previous stage. In this case, we can use Point Cloud based method for the rapid generation of geometries based on point clouds scattered. Generally, there are two algorithmic methods available in PhotoScan that we can apply for the generation of 3D meshes: Field Height - for the type planar surfaces, or Arbitrary - for each object type.

4. After building the polygonal network, it may be necessary to adjust them. PhotoScan is able to make some corrections, such as decimation of the mesh, the removal of isolated components, the closing of holes, etc. When we pursue a more complex and detailed editing, a professional editing software has to be used. In this regard, PhotoScan allows exporting the mesh and to edit it with another software and then reopen it in PhotoScan through the most common interchange formats.

5. After that we reconstructed the geometry (and hence the mesh), we can structure it and/or use it for producing orthophotos.

6. Finally, we need to scale the 3D model starting from a known measurement

However, even if the pattern obtained with SfM was apparently comparable to the laser, though with less precision, to a careful analysis appeared some voids probably due to the quality of the images acquired with the internal chamber of the laser scanner. In the use of the SfM, in fact, is of considerable importance the quality of digital images both in terms of

resolution, but especially in the acquisition mode, which requires the absence of excessive contrasts and therefore uniformity in terms of illumination, and then the overlap between a part of photos with that of the next photo. For this reason, we have focused this discussion exclusively on integrated use of TLS and thermography.

IV. CASE STUDY

In the case under study were acquired images of two different cars (Fig. 3, Fig. 4).

They are a Fiat Punto and a Peugeot 206, the first damaged the left rear, the second on the front left.



Fig. 3 - Fiat Punto crashed in the area of the rear bumper left

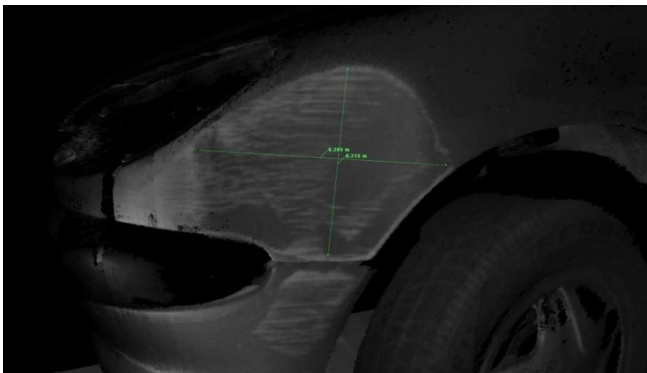


Fig. 4 - Peugeot 206 crashed in the front left side of the headlight

Once simulated the packaging (Fig. 5), on each of them were placed three targets, distributed homogeneously on the surface of interest.

The 3D survey with the laser scanner Leica HDS 3000 of the wall was carried out by two acquisitions from different points of stationing to limit the shadow zones, with a sampling step of 5 mm and a laser scanner - car distance of about 5 m: were thus obtained two point clouds.

The three targets were scanned in detail with the laser scanner and below, images were acquired in the range of infrared cameras Flir B2 with the camera at a distance camera - car about 2 m.



Fig. 5 - Simulation package on two cars

After roto-translating the coordinates of the points of the scans acquired in the local frame of reference of the support points, from the final 3D model (in *MeshLab* software environment), was performed a triangulation that provided a continuous surface of mesh type. With the software *RapidForm*, after highlighting the coordinates of the target as recognizable geometric reference entities on the mesh, we proceeded with the texturing of the image.

The texturing with IR images was carried out through the manual recognition of the 3 target identified in the mesh as reference geometry and the thermal image with a color indicating the points that are cooler than the surface (thanks to the expedient of ice spray used before the acquisition with the thermal camera, Fig. 6).

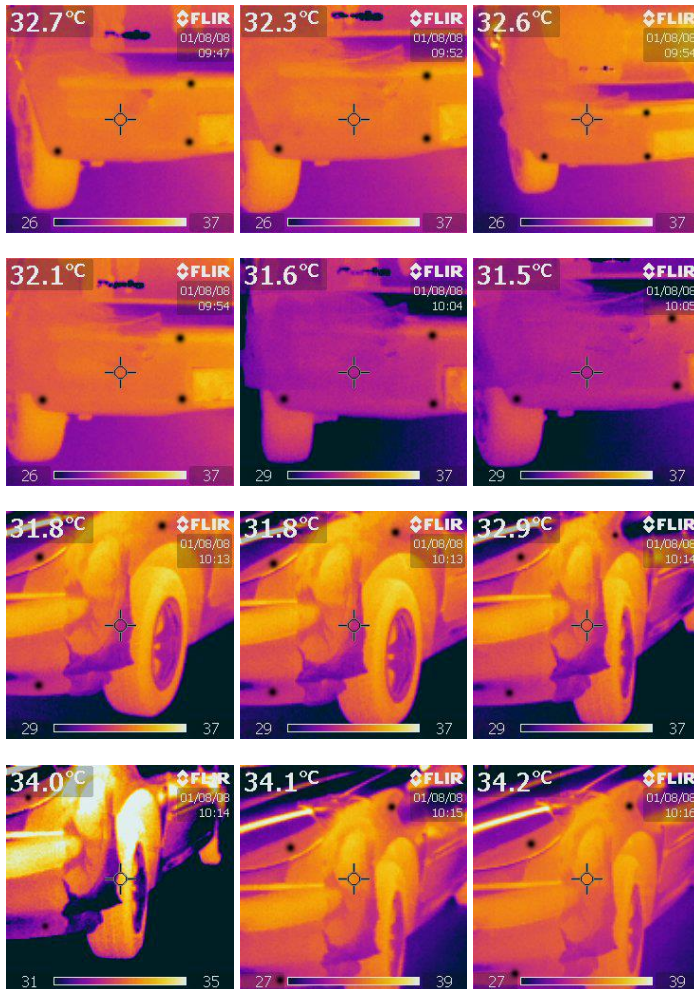


Fig. 6 - Reference image

The texturing was then carried out using the laser scanner target: were not used natural points (such as edges, references the wheels) precisely because of the difficulty of finding the same point in the thermal image and in the triangle mesh. As emphasized by the below images (Fig. 7), the integration of point clouds obtained by laser scanner and thermal imagery provides accurate information on the progress of morphometric alterations characterizing the damage due to accidents. The color distribution in the thermal images and precise alteration of the same is evident proof of the presence of damage. However, the only thermal images cannot be considered sufficient for a reliable estimate of the state of the object under investigation.

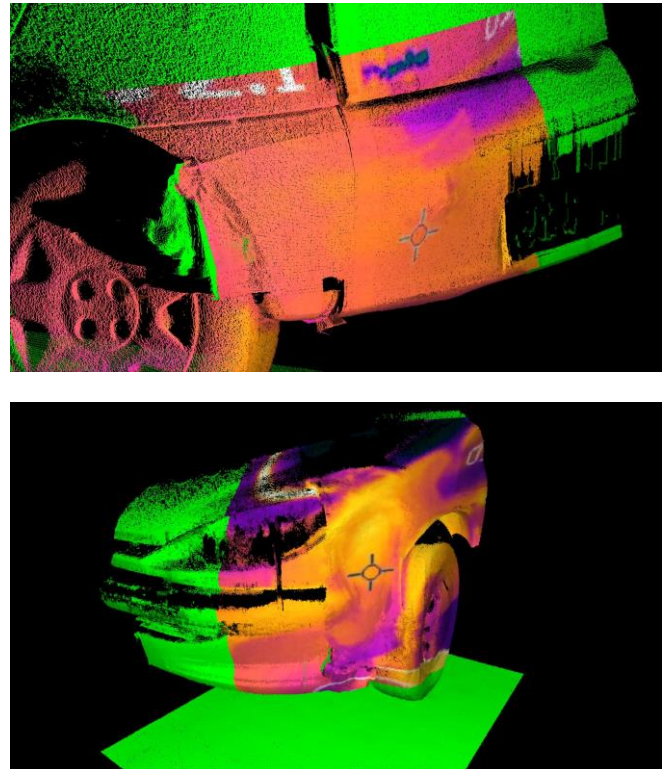


Fig. 7 - Texturing of the images in the infrared range, with a resolution of 800 x 600 pixels

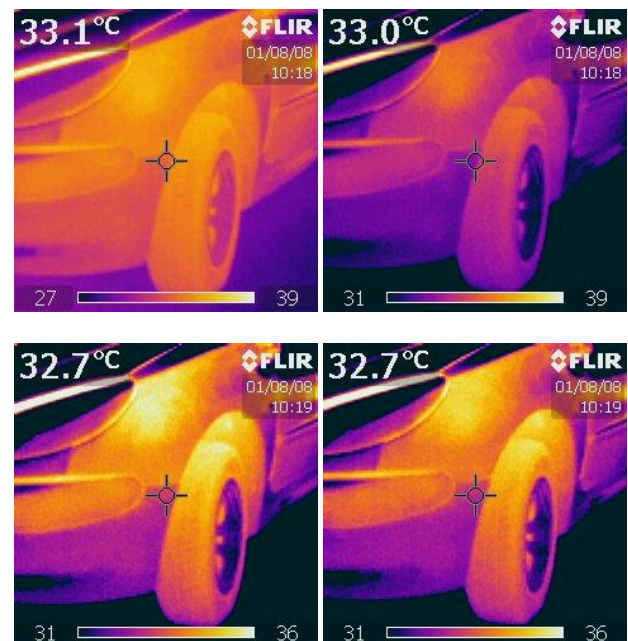


Fig. 8 - Reference image Peugeot 206

For information purposes, we report the thermographic images (Fig. 8) of one of the two cars investigated (Peugeot 206) in undamaged condition, to facilitate a more simple assessment of discoloration found to take over the damage.

V. CONCLUSIONS

The limit of the texturing is in the fact that it is not an automated procedure [8] –[9]; however, the results confirmed the applicability and the validity of the methodology that allows performing the texturing of thermal images on mesh surfaces produced by laser scanning point clouds, which highlighted texture mapping of good quality.

As regards the use of SFM, although in this study it has not provided satisfactory results, we intend to continue the experiment with the use of images with a resolution and suitable operating procedures. In fact, even if the TLS provides further accuracies, the use of the SFM has the advantage of being characterized by a greater speed and allows to realize 3D models at low cost and with a highly automated procedure.

REFERENCES

- [1] A. Rizzi, F. Voltolini, F. Remondino, S. Girardi, L. Gonzo, "Optical measurement techniques for the digital preservation, documentation and analysis of cultural heritage" in *Proceedings of the 8th Conference on Optical 3D Measurement Techniques*, ETH Zurich, Switzerland, 2007, pp. 16-24.
- [2] F. Voltolini, A. Rizzi, F. Remondino, S. Girardi, L. Gonzo, "Integration of non-invasive techniques for documentation and preservation of complex architectures and artworks" in *Proceedings of ISPRS International Workshop 3D-Arch: "3D Virtual Reconstruction and Visualization of Complex Architecture"*, Zurich, Switzerland, 2007.
- [3] C. Achille, R. Brumana, F. Fassi, H. Tuncer, "Application of mixed techniques for the 3D modelling of the noble floor of the Villa Reale in Monza" in *Proceedings of the XXI CIPA Conference AntiCIPAting the Future of Cultural Past*, held in Athens, Greece, 2007.
- [4] U. Stilla, J. Kolecki, L. Hoegner, "Texture mapping of 3d building models with oblique direct geo-referenced airborne IR image sequences" in *Proceedings of ISPRS Workshop: High-resolution earth Imaging for geospatial information 1*, 2009, vol. 38 (1-4-7/W5).
- [5] F. Remondino, A. Pelagotti, A. Del Mastio, F. Uccheddu, "Novel data registration techniques for art diagnostics and 3D heritage visualization" in *Proceedings of the IX Conference on Optical 3D Measurement Techniques*, vol. 1, Vienna, 2009, pp. 1-3.
- [6] F. Uccheddu, A. Del Mastio, A. Pelagotti, F. Remondino, V. Cappellini, "Texture mapping of flat-like 3D models" in *Proceedings of 16th Int. Conference on Digital Signal Processing (DSP 2009)*, Santorini, Greece, 2009, pp. 1-6.
- [7] V. Barrile, G. M. Meduri, G. Bilotta, "Laser scanner surveying techniques aiming to the study and the spreading of recent architectural structures" in *Proceedings of the 2nd WSEAS International Conference on Engineering Mechanics, Structures and Engineering Geology, EMESEG '09: "Recent Advances in Engineering Mechanics, Structures and Engineering Geology"*, Rodos, Greece, July 22-24, 2009, pp. 25-28.
- [8] A. Rizzi, F. Voltolini, S. Girardi, L. Gonzo, F. Remondino, "Digital preservation, documentation and analysis of paintings, monuments and large cultural heritage with infrared technology, digital cameras and range sensors", *International Archives of the Photogrammetry, Remote Sensing and Spatial Information Sciences*, vol. 36, Part5/C53, 2007, pp. 631-636.
- [9] V. Barrile, G. Bilotta, G. M. Meduri, "Archaeological Investigations with TLS and GPR Surveys and Geomatics Techniques", in *Towards Horizon 2020 - Proceedings of 33rd EARSeL Symposium 2013* 3-6 June 2013, Matera, Italy, pp. 857-864.